Photoacoustic microscopy by photodeformation applied to thermal diffusivity determination

Daniel Balageas, Daniel Boscher, Alain Déom, Franck Enguehard

PHOTOACOUSTIC MICROSCOPY BY PHOTODEFORMATION APPLIED TO THERMAL DIFFUSIVITY DETERMINATION

D. L. Balageas, D. M. Boscher, A. A. Déom and F. Enguehard
Division de Thermophysique
Office National d'Etudes et de Recherches Aérospatiales (ONERA)
BP 72 F-92322 Châtillon Cedex, France

Abstract

The photoacoustic method by photodeformation permits to elaborate imagery at micrometer scale. It may be used for nondestructive testing, especially in the microelectronics industry. A quantitative application of this method allowing the relative measurement of thermal diffusivity of samples of some tens μm^3 volume is presented. The measure is relative because it necessitates a reference sample of known diffusivity. Possible applications are : thin films, very small homogeneous samples, samples presenting severe gradients of thermal properties, thin coatings... Some results are presented which concern bulk materials and diamond-like carbon thin coatings.

1 Introduction

Among the various photoacoustic and photothermal methods, the photoacoustic microscopy by photodeformation, proposed for the first time in 1983 (Opsal et al., 1983), has been relatively scarcely used for qualitative or quantitative non destructive evaluation (NDE) and characterization. Let us mention the work of Welsh et al. (1988) who used the method for measurement of the low-absorption of optical thin film. The photothermal method by photoreflectance (Rosencwaig et al., 1985) seems more extensively used now, mainly for microelectronics NDE. Nevertheless, the photoacoustic method by photodeformation which necessitates an experimental arrangement quite similar to the photoreflectance set-up, may be used for obtaining good images at the micronic scale as demonstrated previously by the authors (Déom, Boscher and Balageas, 1990 ; Déom, Boscher, Noirot, Enguehard et Balageas, 1990). The possibility of using this method not only for qualitative characterizations, but for a quantitative determination of thermal properties is here demonstrated. A novel method for diffusivity measurement is proposed which may be applied to bulk materials but also to thin coatings.

2 Principle of photoacoustic method by photodeformation

The principle of the method is illustrated on figure 1. The surface of the sample is heated by a laser beam modulated in amplitude (pump beam). The local heating induces a local deformation of the surface modulated at

the same frequency. If the heating is focused, the surface deformation is enough important and can be used to do characterization. A second laser beam, parrallel to the pump beam is reflected on the surface. The modulation of the reflection angle induces a modulation of the position of the reflected laser beam which is monitored by a position detector. In this method, the aim of the modulation is to decrease the experimental noise by using a lock-in amplifier. The amplitude and phase of the signal can be used for identification of optical, thermal and mechanical properties of the volume of sample excited by the pump beam. This volume depends on the frequency modulation *f*. The length of diffusion of the thermal wave, δ_{th}, with a unidimensional approximation and a homogeneous and opaque material, is related to *f* by the expression $\delta_{th} = \sqrt{\kappa/\pi f}$. κ is the diffusivity of the material : $\kappa = k/C$, with k the thermal conductivity and *C* the volumic heat of the material.

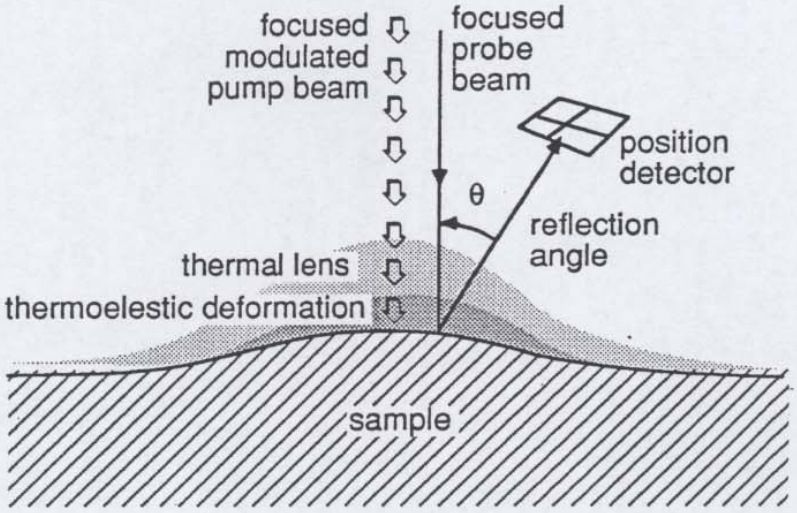

Figure 1. Principle of photoacoustic microscopy by photodeformation.

3 Theory

The measured deflection of the probe beam is the sum of two contributions : the change in the local slope of the surface and the thermal lensing due to the temperature induced index gradient in the air above the sample. In fact, the latter may be neglected - see (Opsal, Rosencwaig and Willenborg, 1983). When the pump beam is modulated, the surface deformation and hence the deflection angle may be splitted into stationary and modulated parts. The measure deals with the modulated part of the signal.

A model was done for prediction of the signal behaviour and identification of the governing parameters. This 2-D model assumes the sample homogeneous, semi-infinite, with an absorption following the Bouguer-Lambert law and optical, thermal and mechanical properties not depending on the temperature. The deformations are assumed weak (no

feedback of the deformations on the heating). The pump beam is supposed Gaussian with radius r_o and power I_o, modulated at the frequency f. The problem necessitates solving the heat equation and the equation of propagation of elastic waves using the Hankel transform.

With these assumptions the following solution is found for the normal deformation U_Z of the surface :

$$U_z(0,r,t) = \frac{\gamma}{\lambda+2\mu}\,\frac{\alpha^2 I_o}{2\pi k}\, e^{j\omega t} \int_0^{\infty} \beta J_o(\beta r)\, \frac{e^{-\beta^2 r_o^2/4}}{\alpha^2 - \beta^2 - j\omega/\kappa}\, x$$

$$\left[\frac{j\sqrt{q^2-\beta^2} - \sqrt{\beta^2 + j\omega/\kappa}}{\sqrt{\beta^2 + j\omega/\kappa}\,(q^2 + j\omega/\kappa)} - \frac{j\sqrt{q^2-\beta^2} - \alpha}{\alpha\,(\alpha^2 + q^2 - \beta^2)} \right] d\beta$$

and the local slope which is half time the deflection angle :

$$(dU_z/dr)_{z=0} = \frac{\gamma}{\lambda+2\mu}\,\frac{\alpha^2 I_o}{2\pi k}\, e^{j\omega t} \int_0^{\infty} \beta^2 J_1(\beta r)\, \frac{e^{-\beta^2 r_o^2/4}}{\alpha^2 - \beta^2 - j\omega/\kappa}\, x$$

$$\left[\frac{j\sqrt{q^2-\beta^2} - \alpha}{\alpha\,(\alpha^2 + q^2 - \beta^2)} - \frac{j\sqrt{q^2-\beta^2} - \sqrt{\beta^2 + j\omega/\kappa}}{\sqrt{\beta^2 + j\omega/\kappa}\,(q^2 + j\omega/\kappa)} \right] d\beta$$

In these expressions $\gamma = (3\lambda + 2\mu)\,\chi$ with χ the linear dilatation coefficient and λ and μ the Lamé coefficients, α is the absorption coefficient, k the thermal conductivity, $q = \omega/v_l$ with v_l the longitudinal wave celerity and J_0 and J_1 are the cylindrical Bessel functions of order zero and -1.

In the restrictive case of an opaque solid ($\alpha \to \infty$) with high elastic length ($q \to 0$) the expression of the slope is simplified :

$$(dU_z/dr)_{z=0} = \frac{1+\sigma}{1-\sigma}\,\frac{\alpha I_o}{2\pi k}\, \chi\, e^{j\omega t} \int_0^{\infty} \beta^2 J_1(\beta r)\, e^{-\beta^2 r_o^2/4}\, x$$

$$\frac{\sqrt{\beta^2 + j\omega/\kappa} - \beta}{j\omega/\kappa\,\sqrt{\beta^2 + j\omega/\kappa}}\, d\beta \qquad (1)$$

with α the absorptivity and σ the Poisson coefficient.

The present model was used for simulating the experience with Al and other materials like Ge that can be considered as opaque. The amplitude of the normal deformation $U_z(r)$ obtained for an Aluminum sample is presented in Fig. 2. The pump beam radius is 3 μm and the absorbed power, αI_o, 5 mW. The deformations are weak, of the order of some Å. In the area directly irradiated by the laser the deformation is mainly influenced by the energy distribution in the beam (here a Gaussian), but for higher radius it is mainly dependent on the thermal length. The slope $dU_z/dr|_{z=0}$ (r) corresponding to these deformations is given in Fig. 3 for frequencies ranging from 2 kHz to 20 MHz. The slope are of the order of some μrad. The corresponding reflection angles are then easily measurable. For thermal diffusion length higher than the beam radius the maximum of the slope is reached at a radius near of *1.1* r_o.

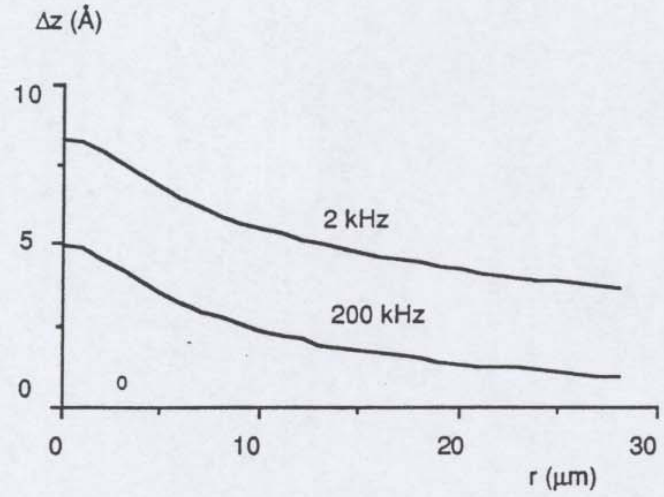

Figure 2. Deformation of an Al sample illuminated by a modulated gaussian-shaped laser beam of 3 μm-radius and absorbed power of 5 mW (numerical simulation results).

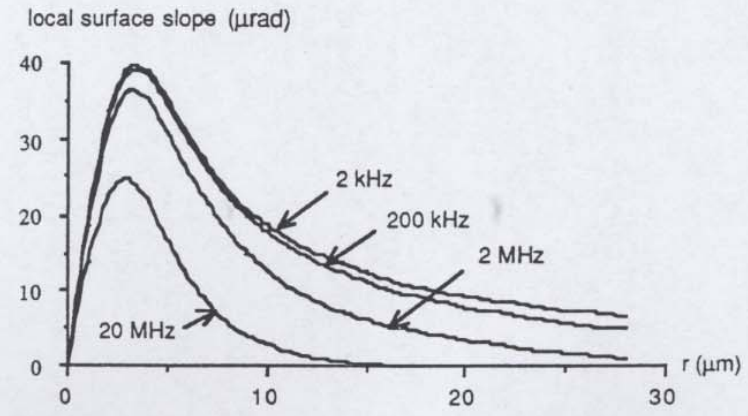

Figure 3. Surface slope of an Al sample illuminated by a modulated gaussian shaped laser beam of 3 μm-radius and absorbed power of 5 mW (numerical simulation results).

The influence of the modulation frequency is presented in Fig. 4 where he slope at $r = r_o$ is plotted versus f, for the same absorbed power and a 5 µm pump beam radius. A plateau is obtained for low frequencies, with a value of the slope equal to :

$$(dU_z/dr)_{max} = [\chi \alpha I_o (1+\sigma)] / [(1-\sigma) 2\pi k]$$

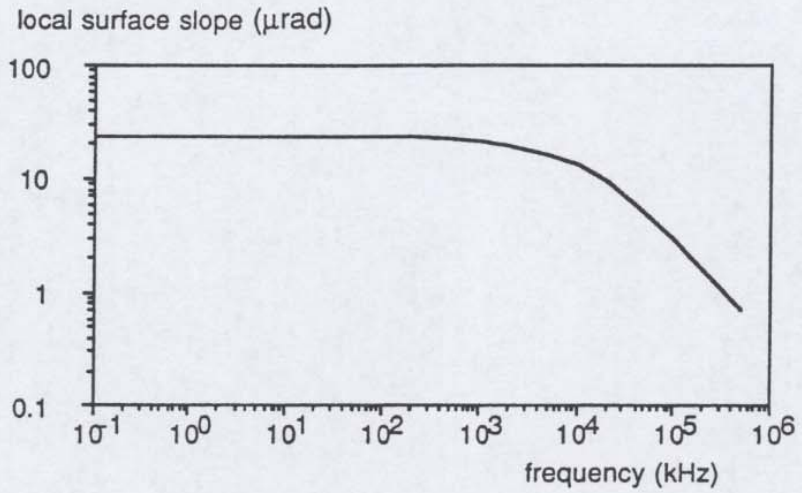

Figure 4. Surface slope at radius location $r_{meas}=r_o$ = 5 µm of an Al sample illuminated by a modulated gaussian-shaped laser beam of 5 µm-radius and absorbed power of 5 mW (numerical simulation results).

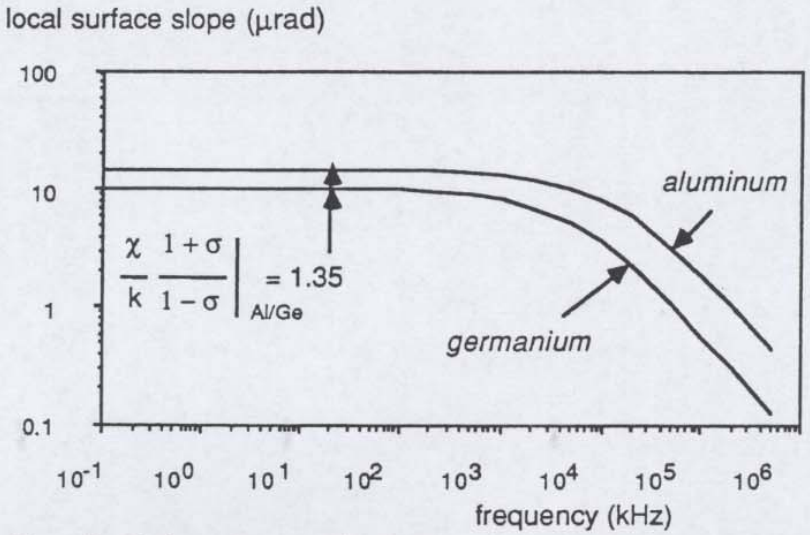

Figure 5. Surface slope at radius location $r_{meas}=r_o$ = 5 µm of two samples of Al and Ge, illuminated by a modulated gaussian-shaped laser beam of 5 µm-radius and absorbed power of 5 mW (numerical simulation results).

This asymptotic value is dependent on both optical, thermal and mechanical parameters. The influence of the material properties is demonstrated in the Fig. 5 where the results corresponding to Al and Ge are compared.

4 Thermal diffusivity determination

If the low frequency signal is used for normalizing the frequency curve $dU_z/dr\big|_{z=0}(f)$ obtained at a given radius, r_{meas}, for an opaque sample the resulting curve is just dependent on the thermal diffusivity of the material:

$$\left.\frac{(dU_z/dr)}{(dU_z/dr)_{max}}\right|_{r=r_{meas}} = \int_0^{\infty} \beta^2 J_1(\beta r_{meas})\, e^{-\beta^2 r_o^2/4}\, \frac{\sqrt{\beta^2 + j\omega/\kappa} - \beta}{j\omega/\kappa\ \sqrt{\beta^2 + j\omega/\kappa}}\, d\beta \qquad (2)$$

Then the amplitude of the reflection angle θ, normalized by its maximum obtained at low frequencies, is a function of a unique parameter, the thermal diffusivity κ :

$$\theta/\theta_{max}\,(\omega) = f(\kappa, r_{meas}, r_o)\ .$$

This is clearly shown in figure 6 where the curves of figure 5 are plotted after normalization.

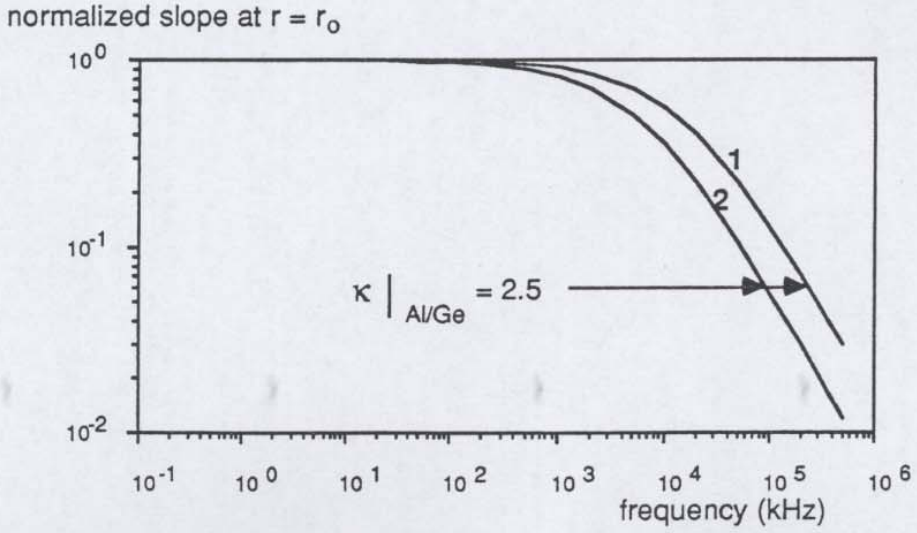

Figure 6. Normalized slope at radius location $r_{meas}=r_o$ = 5 μm of two samples of Al (curve 1) and Ge (curve 2) - numerical simulation results.

Thus, in the case of an opaque sample, the normalization offers the advantage of eliminating the influence of the optical parameters (α, I_o), the mechanical properties (σ, χ) and stationary-regime thermal property (k) of the sample.

There are two possibilities of determining the diffusivity :

i) an absolute determination by fitting the experimental curve $\theta/\theta_{max}(\omega)$ with the theoretical expression (2) which assumes, concerning the experimental arrangement, that the pump beam is gaussian and the probe beam has a negligible extension.

ii) a relative determination by comparing the experimental curves $\theta/\theta_{max}(\omega)$ obtained successively with a reference sample of known thermal diffusivity and a sample of unknown thermal diffusivity. In such a procedure the quality of the pump and probe beams do not need to be known but it is mandatory to maintain them identical during all the experimentation. Furthermore the assumption of opacity and high elastic length must be verified by the two samples.

Finally the linear expansion coefficient of the two samples must be sufficiently high to maintain the deflection of the probe beam by the thermal lens created in the surrounding air negligible comparatively to the reflection angle. In effect, as shown by Opsal et al. (1983), the ratio of the angle of deflection in the air to the angle of reflection on the surface is frequency dependent and maximum for low frequencies. For the low frequency limit its value may be simply evaluated with the following expression :

$$\theta_{defl} / \theta_{refl} = \frac{2}{n}\frac{dn}{dT}\frac{1-\sigma}{1+\sigma}\frac{1}{\chi} \approx \frac{1-\sigma}{1+\sigma}\frac{1.1\,10^{-6}}{\chi}, \qquad (3)$$

where *n* is the index of refraction. In fact, nonlinear effects occur due to high temperatures locally created that tend to reduce this ratio. In table I values of this ratio are given for Al, Ge, Si and diamond. In fact the model does not apply to this last material which is not opaque at the wavelength of the pump beam used (YAG laser), but its properties represent an extreme limit of possible properties generally encountered. In the case of diamond, the contribution of the air lens would be 61 % of the total signal. Even for Si, with a contribution of 33%, this phenomenon impedes the use of the rather simple model described here. For Al (4%) and even for Ge (18%) the method can be applied, especially as the contribution of the air lens is decreasing with increasing frequencies and is over-estimated due to the existence of non linear effects not taken into account here (see Opsal et al., 1983).

A practical way of doing the identification consists in finding the translation vector that leads to a good global superposition of the two experimental curves plotted in semilog coordinates (see figure 7). This vector gives directly the diffusivity ratio of the two samples. This method is applied in figure 6 where the ratio of diffusivity of Al and Ge, equal to 2.5 (see table I), is graphically identified.

Materials Physical properties	Symbols	Diamond	Si	Al	Ge	Al/Ge
Poisson ratio	σ	0.16	0.28	0.35	0.35	
Linear expansion coeff. (K^{-1})	χ	$1.0\ 10^{-6}$	$2.5\ 10^{-6}$	$2.5\ 10^{-6}$	$5.7\ 10^{-6}$	
Thermal conductivity ($Wm^{-1}K^{-1}$)	k	$2.6\ 10^{3}$	$1.6\ 10^{2}$	$2.2\ 10^{2}$	$5.9\ 10^{1}$	
Volumic heat ($Jm^{-3}K^{-1}$)	C	$1.8\ 10^{6}$	$1.6\ 10^{6}$	$2.4\ 10^{6}$	$1.6\ 10^{6}$	
Thermoelastic coupling factor	$\gamma = \chi(1+\sigma)/(1-\sigma)$	$1.4\ 10^{-6}$	$4.5\ 10^{-6}$	$5.1\ 10^{-5}$	$1.0\ 10^{-5}$	
Signal governing parameters						
Slope at low frequencies ~	γ/k	$5.4\ 10^{-10}$	$2.8\ 10^{-8}$	$2.3\ 10^{-7}$	$1.7\ 10^{-7}$	*1.35*
Thermal diffusivity (m^2s^{-1})	$\kappa = k/C$	$1.4\ 10^{-3}$	$1.0\ 10^{-4}$	$9.2\ 10^{-5}$	$3.7\ 10^{-5}$	*2.50*
Maximum contribution of air lens to total signal (%)	from eq. (3)	61 %	33 %	4 %	18 %	

Table I. Compared physical properties and parameters governing the signal for Al, Ge, Si and diamond

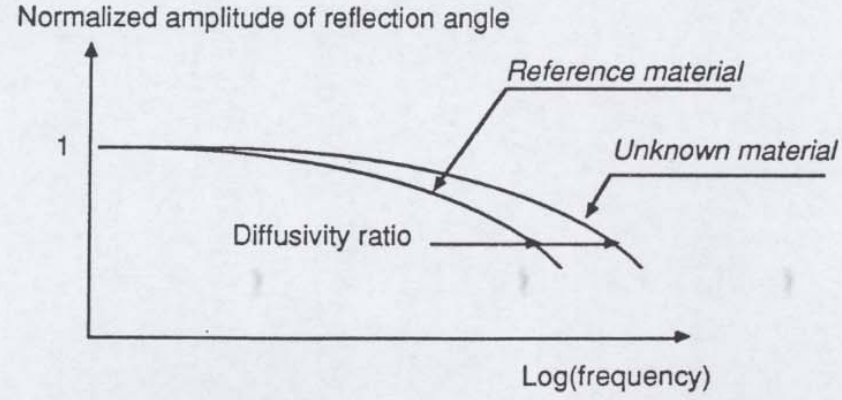

Figure 7. Principle of diffusivity determination by relative measurements. Pump beam and radial location of the probe beam must be kept identical for the two set of measurements.

5 Experimental set-up

The experimental arrangement is shown in figure 8. The heating beam is obtained by modulating with an acousto-optic modulator a CW laser beam delivered by a Nd-Yag laser (λ =1.06μm), running in single mode, the beam being gaussian and 1.5 mm in diameter. The diaphragms allow the first-order beam to be selected with a modulation factor close to 100%. The beam splitter reflects 8% of the main beam which allows the knowledge of the incident power on the sample. The dichroïc filter is transparent for the pump beam but reflects the probe beam. The microscope objective, with a numerical aperture n_a equal to 0.65 allows theoretically a diameter of the pump beam at the surface of the sample equal to λ/n_a = 1.6 μm. The sample is attached to two orthogonal step stages. It is thus possible to obtain an image with a minimum value of 0.1 μm between each step. The stages are driven by an electronic system which is connected to a microcomputer. The probe laser is constituted by a He-Ne laser (λ =0.633 μm), with a power equal to 2 mW and a beam diameter equal to 0.65 mm. Behind the microscope objective the probe beam is equal theoretically to λ/n_a = 1 μm. In fact, the measured diameters were near of 3 μm for both pump and probe beams (Déom, Boscher, Noirot, Enguehard et Balageas, 1990). The polarization-beam-splitting cube transmits the part of the beam polarized vertically. The quarter-wave retarder transforms the linear polarisation of the beam in an elliptical one. After reflection on the sample, the beam becomes horizontally polarized across the quarter-wave retarder and is reflected on the polarization-beam-splitting cube. An interferential filter eliminates a possible residual beam at λ = 1.06 μm coming from a reflection on the sample of the pump beam. The position detector is a silicon 4-quad detector, 9.65 mm in diameter, with a detectivity equal to 3.1 10^{-12} cm $Hz^{1/2}$ W^{-1} for

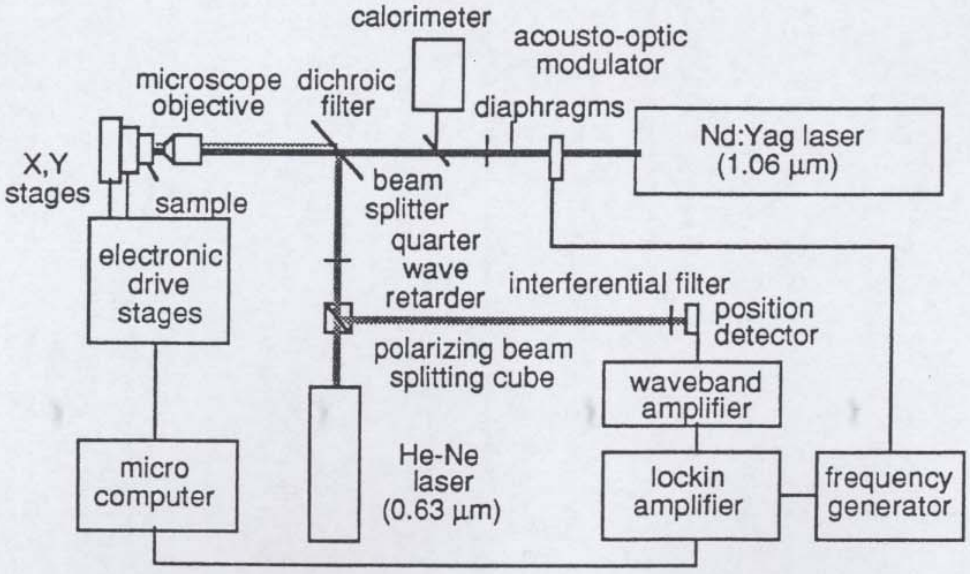

Figure 8. Experimental set-up.

λ = 0.633 μm. Its response time is about 80 ns. The wave-band amplifier was built at ONERA. For two opposite quads, it gives a tension proportional to the displacement of the beam in the direction of the two quads. Its bandpass is equal to 3 MHz. The lock-in amplifier can work between 0.1 and 50 MHz. Its reference input is connected to the frequency generator. The total sensivity on the detector is 30 Å, which corresponds to an angle equal to 2 nrad on the sample. The stages and the output of the lock-in amplifier are connected to a Victor Sirius microcomputer which controls the experiment. The microcomputer orders the stages to translate one or several steps vertically or horizontally and, for each position, records the two outputs of the lock-in amplifier corresponding to the amplitude and the phase of the signal.

The position of the probe beam with regards to the deformation of the surface of the sample is adjusted by translating the He-Ne laser and by rotating the dichroic filter. For the low frequencies, the distance r between the axes of the probe beam and of the pump beam must be equal to 1.1 time the radius of the pump beam for obtaining the maximum value of the signal (Opsal et al.,1983). For high frequencies, the maximum is obtained for r=0.7 time the radius of the pump beam.

6 Results concerning absolute determination of homogeneous samples diffusivity

The first experiments were done with a 1mm-thick polished Al sample. The evolution of signal to noise ratio for this material is given in figure 9 for frequencies ranging from 3 kHz to 1 MHz. The signal/noise ratio is decreasing with increasing frequencies. The values of the slope of the sample surface, and thus of the reflection angle detected by the position detector, are very low (some tens of nrad). They were obtained with an incident power of 86 mW corresponding to an absorbed power of 3.4 mW.

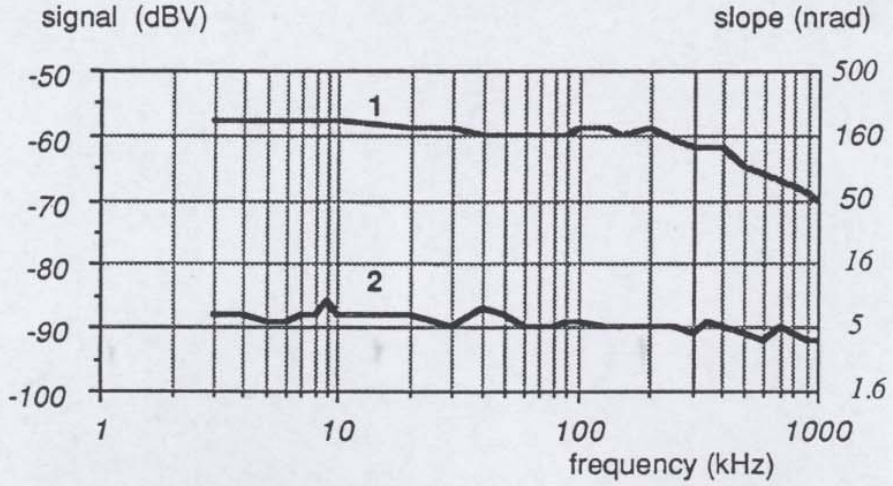

Figure 9. Signal obtained with an Al sample (curve1) and corresponding noise (curve 2).

The experimental frequency response of the aluminum sample was compared to the theory (see figure 10). There is an important discrepancy between the two curves. Among the possible causes of discrepancy let us mention : the fact that the pump beam diameter was in the present case equal to 8 μm (compared to 5 μm for the theoretical results), the finite diameter of the probe beam which is assumed negligible in the theory, the difficulty to know the exact relative position of the two beams, the assumption of constant thermal and mechanical properties for Al in spite of the thermal heating created in the sample, and finally the existence of a deflection of the probe beam by the air lens. It was concluded that the adequation of the theoretical model to the real experimental conditions is difficult. Correlatively the absolute identification of the thermal diffusivity without the help of a sophisticated model with numerous parameters to identify or to adjust seems impossible.

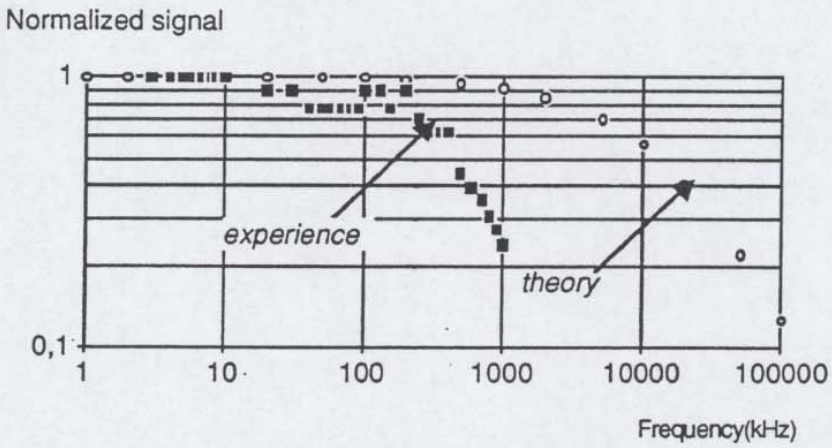

Figure 10. Comparison between theory and experience for Al.

7 Determination of thermal diffusivity by relative measurements

The method of thermal diffusivity determination using a reference sample was applied to Ge, the reference material being Al. The curves obtained with the two Al and Ge samples, using the same optical arrangement and same pump laser power of 86 mW are presented in figure 11. On this graph the Al data are plotted after dividing the frequency by a factor of 2.5 equal to the ratio of the diffusivities of Al and Ge. This operation gives a global translation of the Al curve in the semilog graph. With such a translation the two experimental curves are superposed. It can be concluded that the determination of the diffusivity by the relative method is possible. More parametric studies and more experiments are needed for determining the accuracy of the method. With the noise obtained with the present set-up the accuracy is certainly not excellent but the main interest of the method which is the possibility of measuring in a very small volume (some tens of μm^3) is sufficiently attractive to counterbalance this poor accuracy.

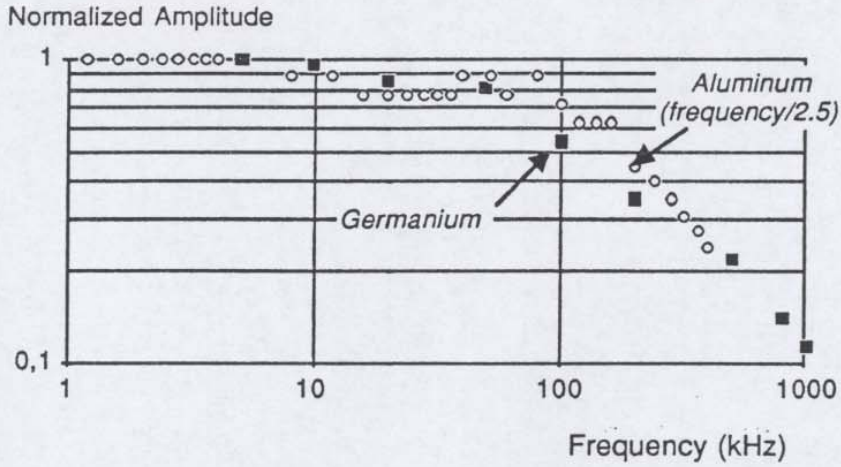

Figure 11. Diffusivity of Ge determined by comparative measurement with Al as reference.

8 Application of the relative method to thin coatings

8.1 Principle of the method

The method can be applied to the characterization of a thin coating on a massive substrate. In this case the substrate is considered as the reference material. The procedure is the following :

i) a first series of measurements is done on a first reference sample. The purpose of this primary reference sample is to obtain the shape of the frequency curve characteristical of the set-up arrangement.

ii) a second series of measurement is done on the coated sample. The frequency excursion must be sufficiently wide-spread for obtaining some data influenced by the coating alone (high frequencies corresponding to thermal diffusion depths, $\delta_{th} = \sqrt{\kappa/\pi f}$ lower than the actual coating thickness) and some data depending on the substrate alone (low frequencies corresponding to δ_{th} much higher than the coating thickness).

iii) the identification is done now using local translations between the unkwnon coated sample curve and the primary reference sample curve. These local translations allow the superposition of small parts of a curve with small parts of the other curve. Thus, for each frequency (and correlatively each δ_{th}) an effective thermal diffusivity is obtained - or more precisely a ratio of an effective diffusivity to the primary reference diffusivity. For high frequencies corresponding to δ_{th} smaller than the actual coating thickness the effective diffusivity curve must present a plateau. The same must occur for the lower frequencies corresponding to δ_{th} much higher than the actual

coating thickness. From the ratio of the effective diffusivities of the two plateaux the coating diffusivity can be determined knowing the substrate diffusivity. In this case the diffusivity of the primary reference sample may be unknown. If the diffusivity of the substrate is unknown, the diffusivities of coating and substrate can be determined from the diffusivity of the primary reference sample.

8.2 Application to a diamond-like carbon coating

The feasibility of the method was demonstrated using a Ge sample with a 2.6 μm-thick diamond-like carbon (DLC) coating. The characteristics of this coating are given by Déom et al. (1985). The primary reference sample used was a bare Ge sample. The normalized signal versus frequency for the two samples are given in figure 12.

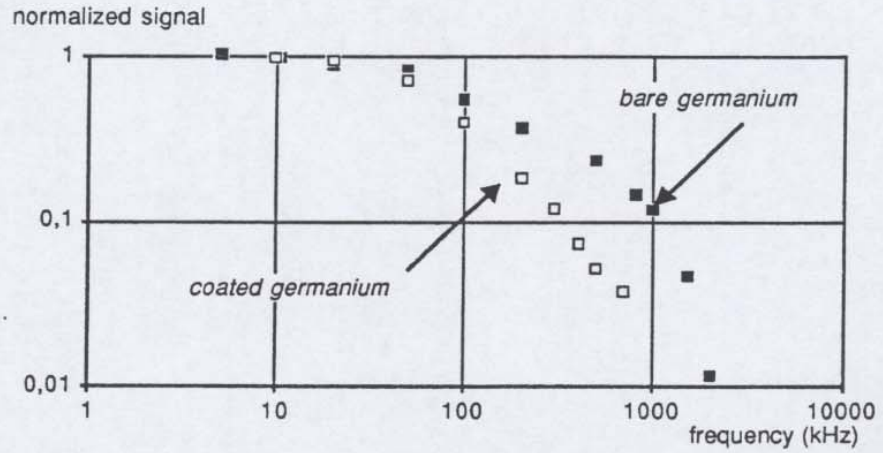

Figure 12. Normalized signal versus frequency for bare Ge and diamond-like carbon coated Ge samples.

In figure 13 the effective diffusivity obtained using the local translation method is given versus the thermal diffusion length calculated using the frequency and the corresponding effective diffusivity. A plateau is effectively obtained for thermal diffusion depths δ_{th} lower than 4 μm (corresponding to frequencies higher than 200 kHz) and a second one for δ_{th} higher than 20 μm (corresponding to frequencies lower than 20 kHz). The ratio of these two plateaux is 0.33 corresponding to a coating diffusivity of 1.2 10^{-5} m^2s^{-1} assuming a diffusivity of Ge equal to 3.6 10^{-5} m^2s^{-1}. The δ_{th} limit (4 μm) corresponding to the end of the coating plateau is near of the actual coating thickness (2.6 μm).

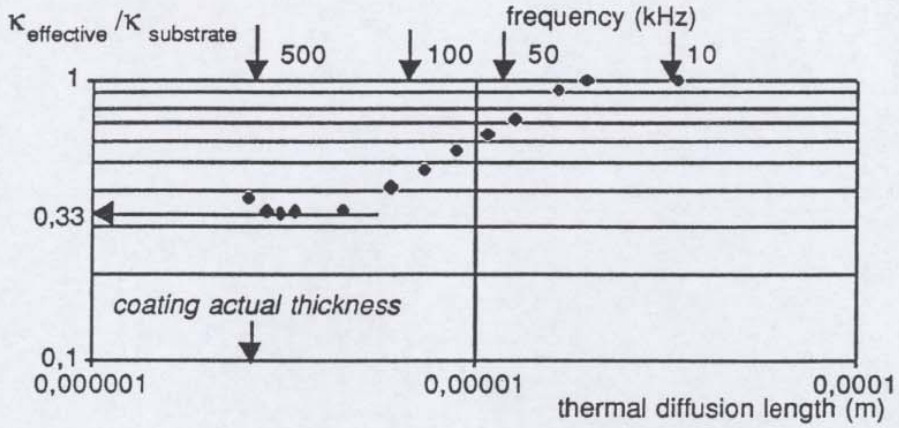

Figure 13. Diffusivity of diamond-like carbon coating with Ge substrate as a reference.

8.3 Importance of the thermal contact resistance of the interface between thin coating and substrate

The transition region of the frequency curve between the two plateaux is dependent on the thermal contact resistance of the coating/substrate interface. This thermal contact resistance could be identified by comparing the experience to a more sophisticated model. Nevertheless, an evaluation of the order of magnitude of the thermal contact resistance is still possible without the help of such a model using both the present result and previous data obtained with the same type of coating using the pulsed photothermal radiometry (Boscher, Déom and Balageas, 1989). The sample used in this first experiment was a sandwich-type sample constituted of three layers :

- a massive Al substrate,
- a 1.1 μm-thick DLC coating,
- a 2.4 μm-thick Al extra-coating.

The front-face thermogram was compared to a simple analytical model considering 3 layers with perfect contact at the interfaces (Balageas et al., 1986). The fitting of the thermogram lead to a value of thermal conductivity k = 2.0 W m^{-1} K^{-1} for the DLC coating. This value was quite insensitive to the volumic heat assumed for the coating (a value intermediate between diamond and graphite values was taken). As concluded in this last reference, the presence of a thermal contact resistance was suspected for explaining the very low value found for the thermal conductivity. In fact this value must be considered as an effective conductivity k_{eff} related to the global thermal resistance R_{eff} of the DLC layer associated with the two thermal contact resistances of the two interfaces (Al coating/DLC coating and DLC coating /Al substrate). Let R be this resistance, assumed typical of the DLC coating and independent of the substrate, the following relation may be stated, δ_{coat} being the coating thickness :

$$R_{eff} = \delta_{coat}/k_{eff} = \delta_{coat}/k_{DLC} + 2\,R$$

$$1.1\ 10^{-6} / 2.0 = 1.1\ 10^{-6} / k_{DLC} + 2\,R \qquad (4)$$

We can evaluate the actual thermal conductivity of the DLC coating, k_{DLC}, from the diffusivity value deduced from the present experiments, assuming a density of 2200 kg m^{-3} and a specific heat of 600 J kg^{-1} K^{-1} (a mean value between the diamond specific heat of 520 J kg^{-1} K^{-1} and the graphite specific heat of 710 J kg^{-1} K^{-1}) :

$k_{DLC} = \kappa \rho C = 1.2\ 10^{-5} \times 2200 \times 600 = 16$ W m^{-1} K^{-1}.

With this value of k_{DLC} relation (4) leads to the following thermal contact resistance :

$R = 2.4\ 10^{-7}$ m^2 K W^{-1}.

This value is very low and characteristic of a very good thermal contact, but is more than three times higher than the thermal resistance of the coating alone which is : $\delta_{coat}/k_{DLC} = 1.1\ 10^{-6} / 16 = 0.69\ 10^{-7}$ m^2 K W^{-1}. It can be concluded that for very thin coatings it is impossible to neglect the thermal contact resistance between coating and substrate. Thus, for determining the thermal properties of the coating two possible ways are possible :

i) if the frequency of the modulated signal is relatively low, or the time delay after a pulse relatively long, the identification must be based on a realistic model taken into account this resistance ;

ii) if no sophisticated model is used, the frequency must be sufficiently high (or the time after the pulse sufficiently short) for giving informations independent of the thermal contact resistance. In this case a rather simple model can be used as done in the present work in which an homogeneous sample model is associated with an effective frequency-dependent diffusivity.

9 Conclusion

The photoacoustic method by photodeformation was presently used for diffusivity determination. Two procedures were proposed : an absolute determination based on the comparison between the experiment and a rather simple model, and a relative determination using a reference sample of known diffusivity. The first method failed, the model being not sufficiently realistic. The second method lead to good results. The improvement of the absolute method using a more sophisticated model is possible but it is not obvious that the results would be better than those obtained with the relative method. In effect, additional parameters are to be taken into account in an improved model, wanting to be predetermined or identified from the experiments. It is too soon to give an estimate of the accuracy reached by the relative method, but it seems not to be high. This fact is offset by the main

interest of the method which is the ability of operating on small volumes of some tens of μm^3.

The method is applied with some modifications to the determination of the diffusivity of a thin coating - here a 2.6 µm-thick diamond-like carbon coating on a Ge substrate. The determination is based on the same simple model assuming an opaque homogeneous sample. From the frequency dependence of the identified effective diffusivity, a value of coating diffusivity is measured knowing the substrate diffusivity. The substrate in this case is the reference material. The diffusivity thus obtained for the diamond-like carbon coating is $1.2\ 10^{-5}\ m^2s^{-1}$. This value must be considered as a first approximate since the coating total opacity for such a thin layer is questionable. Using both the present results and previous data obtained by pulsed photothermal radiometry, the thermal contact resistance of the coating/substrate interface was deduced and found very low ($2.4\ 10^{-7}\ m^2\ K\ W^{-1}$) but higher than the thermal resistance of the coating itself.

References

Balageas D.L., Krapez J. and Cielo P., 1986, J. Appl. Phys., 59, pp. 348-357.

Boscher D., Déom A.A. and Balageas D.L., 1989, High Temperatures - High Pressures, **21**, pp. 113-117.

Déom A.A. , Mackowski J.M. , Balageas D.L. and Robert P., 1985, *Proceedings of the International Society for Optical Engineering*, **590**, pp. 106-109.

Déom A., Boscher D. and Balageas D., 1990, "Micrometer photoacoustic imaging by photodeformation : application to carbon-carbon composites", in *Photoacoustic and Photothermal Phenomena II*, Springer Series in Optical Sciences, **62**, pp.13-16.

Déom A., Boscher, Noirot L., Enguehard F and Balageas D., 1990, "Imaging the interface between fibres and matrix in the yarns of three-directional carbon-carbon composites by a photoacoustic method", in Materials Science and Engineering, B5, Ed. Elsevier Sequoia, pp.135-141.

Opsal J., Rosencwaig A. and Willenborg D., 1983, Appl. Optics **22**, pp.3169-3176

Rosencwaig A., Opsal J., Smith W.L. and Willenborg, 1985, Appl. Phys. Lett. **46**, 1013.

Welsch E., Walther H.G., Eckardt P. and Ton Lan, 1988, Can. J. Phys., 66, pp.638-644.